CARBON-OPTIMIZED BUILDING MASSING WITH CONSTRUCTIVE SOLID GEOMETRY STRATEGIES: A PARAMETRIC MULTI-OBJECTIVE FRAMEWORK

Thanasak Phittayakorn[1] and Chavanont Khosakitchalert[2,*]

Received: September 29, 2025; Revised: October 27, 2025; Accepted: November 17, 2025

Abstract

The early-stage performance of architectural design is critical for long-term carbon optimization. This study investigates three constructive solid geometry (CSG) strategies, namely union, subtraction, and intersection, within a parametric workflow driven by the Non-dominated Sorting Genetic Algorithm II (NSGA-II), aiming to minimize operational carbon emissions (OCE) and maximize gross floor area (GFA). It connects geometric design logic with objectives to support carbon-conscious massing decisions. The study examines how CSG strategies influence simulation runtime, model validity, and design diversity; how NSGA-II optimizes form generation under regulatory constraints e.g., floor area ratio (FAR), open space ratio (OSR); and how these affect early-stage outcomes. Out of 3,000 generated configurations, the subtraction strategy achieved the lowest operational carbon intensity (181.30 kgCO_2eq/m^2 at 45,901.85 m^2 GFA) and provided greater design diversity with 151 valid configurations, while the intersection strategy demonstrated the fastest simulation runtime of 3h 40m 40s. The proposed framework effectively filtered infeasible designs and ensured regulatory compliance to maintain model validity. Convergence of optimal OCE values (~181 kgCO_2eq/m^2) across strategies suggests a useful benchmark for high-rise office buildings in dense urban contexts. These findings highlight the value of integrating carbon optimization, regulatory constraints, and multi-objective parametric design into early-stage architectural workflows to improve sustainability.

Keywords: **Carbon Optimization; CSG Strategies; Early-Stage Performance; NSGA-II; Parametric Design**

[1] *Department of Architecture, Faculty of Architecture, Chulalongkorn University, Bangkok, 10330, Thailand. E-mail: 6471004925@student.chula.ac.th*

[2] *Architectural Intelligence (A.I.) Research Group, Department of Architecture, Faculty of Architecture, Chulalongkorn University, Bangkok, 10330, Thailand. E-mail: chavanont.k@chula.ac.th*

[*] *Corresponding author*

DOI: https://doi.org/10.55766/sujst11660

Introduction

Decisions made during the early stages of architectural design such as conceptual and schematic design significantly influence a building's long-term environmental impact. According to Ciardiello *et al*. (2020), designers at this stage have the greatest flexibility to reduce energy demand by up to 60% and thereby affect operational carbon emissions (OCE) through decisions about building form and shape, which ultimately influence emissions, a major contributor to climate change (Churkina *et al*., 2020; Röck *et al*., 2020). Early adoption of low-carbon strategies is effective because modifications to mass and form are easier, faster, and more cost-efficient. Several studies highlight this stage as a critical opportunity to integrate carbon-conscious strategies into the design workflow (Broyles *et al*., 2024; Dunant *et al*., 2021; Idrissi Kaitouni *et al*., 2025; Parasonis *et al*., 2012).

Despite this opportunity, early-stage massing design presents significant challenges, including design uncertainty, inefficient shapes, and unreliable environmental data (Alkadri *et al*., 2020; Jang *et al*., 2022; Kanyilmaz *et al*., 2023; Pinich *et al*., 2023; Kamel *et al*., 2024). These limitations constrain diverse, high-performance solutions and hinder reliable carbon assessment.

To address these limitations, researchers have increasingly adopted parametric modeling systems integrated with optimization techniques for 3D modeling. Constructive Solid Geometry (CSG), which uses primitive solids combined through Boolean operations such as union, subtraction, and intersection enable the creation of precise volumetric models (Shapiro & Vossler, 1991; Wang *et al*., 2021). This method offers geometric control and computational efficiency, maintaining low memory usage and rapid iteration compared to boundary representation, mesh-based, or voxel-based modeling (Ahmed *et al*., 2016; Huang *et al*., 2020; Mews *et al*., 2024; Ming *et al*., 2016; Wang *et al*., 2021). Integrated with parametric modeling, CSG enhances generative design by allowing systematic exploration and optimization (Wang, 2021; Shapiro & Vossler, 1991). Coupling CSG workflows with multi-objective optimization algorithms, such as the Non-dominated Sorting Genetic Algorithm II (NSGA-II), supports low-carbon building design through the generation of optimized building massing configurations (Deb *et al*., 2002; Torabi *et al*., 2025).

However, generative design research still emphasizes energy and thermal analysis, often limited to specific building types or passive strategies. Attention to 3D modeling methods that enhance form diversity and reliability is limited, and the use of CSG for 3D modeling remains uncommon. Existing tools such as EvoMass (Shen *et al*., 2021; Wang, 2022; Zhang *et al*., 2024) provide strong generative capabilities for early exploration of wind and daylight but lack evaluation of computational efficiency. Recent studies highlight the importance of multi-objective optimization for achieving more sustainable solutions, despite increased complexity (Cruz *et al*., 2024). Integrated frameworks combining generative design, optimization, and LCA show promise but require improved usability and efficiency (Yang *et al*., 2024). Enhancing accuracy and computational performance remains key (Schwartz *et al*., 2021; Shi *et al*., 2025).

Research exists on evaluating CSG operations within generative workflows (Ahmed *et al*., 2013, 2016). For example, structural topology optimization with CSG representation (Huang *et al*., 2020) and mesh-based Boolean operations (Feito *et al*., 2013) have been studied, but systematic evaluation of each operation on indicators such as computational efficiency, structural feasibility, or regulatory compliance remains limited (Ahmed *et al*., 2013; Wang, 2021; Wang *et al*., 2021).

NSGA-II remains a widely adopted evolutionary algorithm in performance-based design due to its capacity to generate Pareto-optimal solutions and maintain population diversity (Deb *et al*., 2002). Lu *et al*. (2022) demonstrated that integrating NSGA-II with building models can reduce computational demand from 1,500 hours to 105 hours (a 93% reduction) while achieving low energy design goals. Zhang *et al*. (2024) reviewed challenges in embedding optimization into urban design workflows and noted that evolutionary algorithms account for 83% of reviewed applications. Nevertheless, its practical utility is limited because NSGA-II often runs as a separate batch process, which slows responsiveness and hinders iterative early-stage use (Guo *et al*., 2023; Zhang, 2024). Moreover, although carbon intensity is a critical metric, it is not widely adopted as a direct optimization objective in early generative processes.

To address these gaps, this study proposes a systematic evaluation of the union, subtraction, and intersection operations within an integrated parametric-optimization workflow that incorporates NSGA-II. The study seeks to answer three key questions: 1) how different CSG strategies influence low-carbon building mass in terms of simulation runtime, model validity, design diversity, and carbon intensity. 2) how NSGA-II can optimize form generation under spatial feasibility and operational carbon emissions. 3) how these strategies contribute to early-stage massing design outcomes. Therefore, the study offers methodological, computational, environmental, and practical contributions by proposing a replicable and performance-informed design approach that supports architects in balancing form generation with sustainability goals at early stages.

Materials and Methods

This study proposes a methodological framework that integrates CSG operations with the NSGA-II. The approach aims to evaluate early-stage massing design using four key performance metrics: simulation runtime, model validity, design diversity, and carbon intensity within a unified workflow. This section presents the proposed method, as seen in Figure 1.

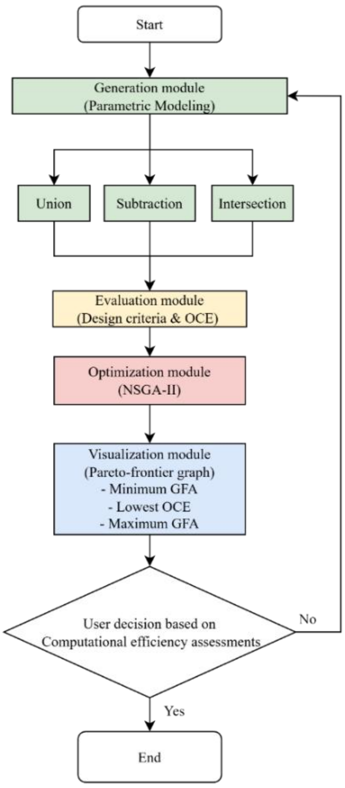

Figure 1. Proposed method

An overview of the proposed method

This research proposes a Parametric System for Assessing and Optimizing Carbon Emissions in Early-stage Building Design (PA-O-CEE) a methodology for early-stage massing design that integrates generative design with NSGA-II to optimize GFA and OCE. The proposed method comprises five modules: 1) Generation Module, 2) Evaluation Module, 3) Optimization Module, 4) Visualization Module, and 5) Computational Efficiency Assessments. These modules provide the conceptual foundation

1. Generation module

The Generation Module defines site boundaries, requirements, climate, context, and codes, enabling parametric modeling and adjustable mass models modified through three CSG strategies. Users define constraints such as height limits and key variables to guide generation. The PA-O-CEE prototype, developed in Grasshopper, a visual programming plugin for Rhinoceros, this process is demonstrated in Figure 1. Rhino is a 3D modeling platform, while Grasshopper enables parametric modeling through a drag-and-drop interface. Building mass is generated through three integrated components: site and building rules, parameters, and CSG-based operations, which together form a unified parametric workflow, as seen in Figure 2.

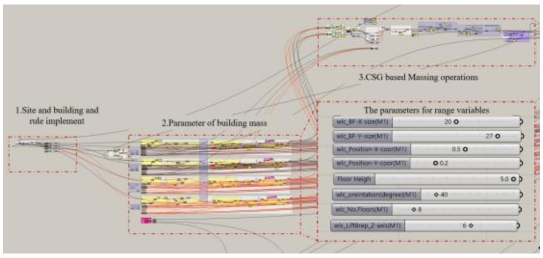

Figure 2. Grasshopper definition for parametric building mass: site input, mass parameters, and massing operations

First, Site and Building rule implementation was modeled in Rhinoceros to define the site dimensions. Surrounding contextual elements, including climate conditions and urban defining position and true north were incorporated to establish site understanding, as seen in Figure 3 (a) site real-world location. Following this, building limit lines and setback boundary lines were defined. This spatial logic is depicted, as seen in Figure 3 (b) Surrounding context and (c) Height restriction. The enclosed area was calculated, providing usable space for construction and functions. Consequently, the 3D model of the site and context was created in Rhino, as seen in Figure 3 d) 3D site real-world location and surrounding context

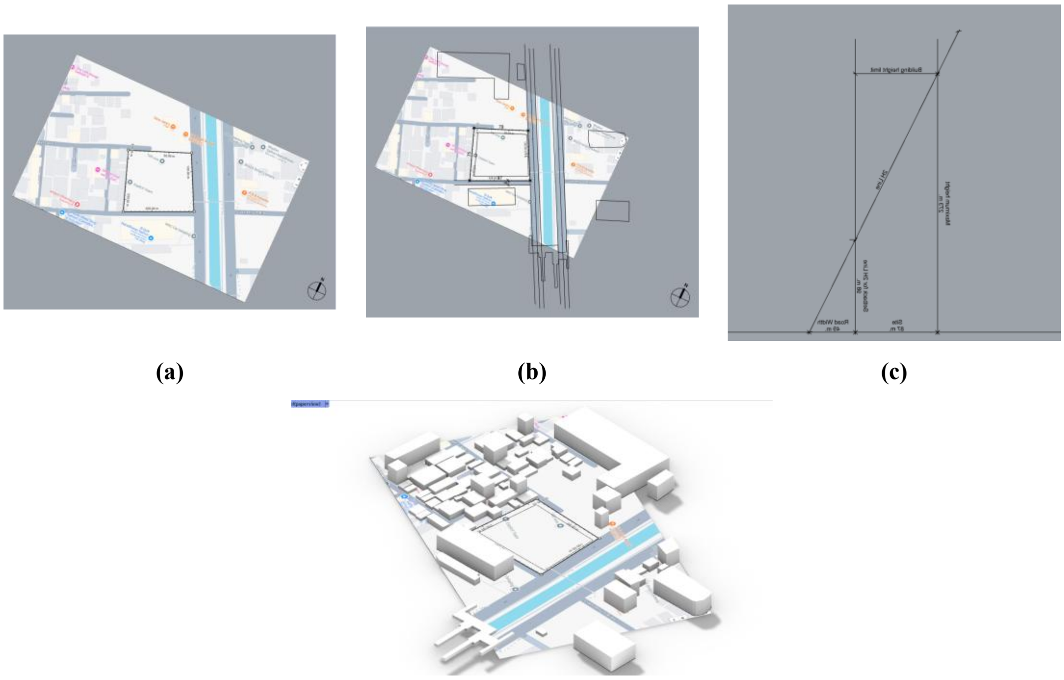

(a) (b) (c)

(d)

Figure 3. Rhinoceros site setup: site location, environmental context, and urban planning regulations

After defining the site boundary, building masses were generated using Grasshopper, a visual programming plug-in for Rhinoceros, as seen in Figure 4(a) Initial platform. The base platform was created within the site setback. A point was placed on a surface subdivided into 1, 2, or 4 points, depending on user controls, to define the building footprint. The width (X) and length (Y) were adjustable, as seen in Figure 4(b) Single-point control, (c)Two-point control, (d) Four-point control.

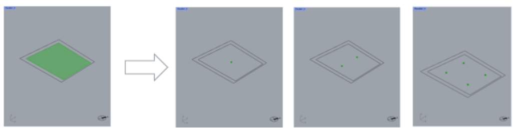

(a) (b) (c) (d)

Figure 4. Generation of building footprints based on setback constraints and control point subdivision

The footprint could move along the X and Y directions within the setback boundary, as seen in Figure 5. The entire building footprint edges within the setback boundary, as seen in Figure 6(a) Centralized footprint. However, any building footprint exceeding the setback were automatically trimmed if no more than two edges exceeded the boundary, as seen in Figure 6(b)Shifted footprint. The building footprint formed the floor plate, extruded to create the vertical mass, as seen in Figure 6(c) Resulting vertical mass.

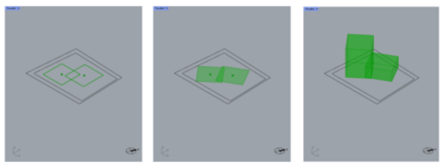

Figure 5. Footprint translation within setback boundaries and initial extrusion

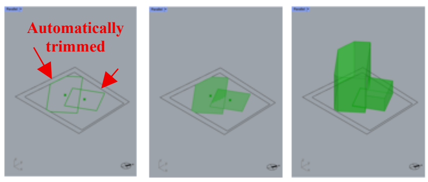

Figure 6. Automated trimming of excess mass beyond allowable setback edges

Additional adjustments were made to the building mass based on floor height, orientation angle, and vertical transformation along the Z-axis to generate various configurations as seen in Figure 7(a) and Figure 8(a) Floor plates. Window and exterior wall elements were derived from extruded floor plates as seen in Figure 7(b) and Figure 8(b)Windows and the WWR was adjustable as seen in Figure 7(c) and Figure 8(c)Walls. In this study, a constant WWR of 0.90 was applied to all facades to isolate the effect of building mass on OCE. The decision was reflected orientation's critical role in shaping form and energy performance. As such, orientation was selected as the initial variable for analysis before other factors (Wang *et al.*, 2024). Lastly, the roof was selected from the topmost plate, as seen in Figure 7(d) and Figure 8(d) Roof.

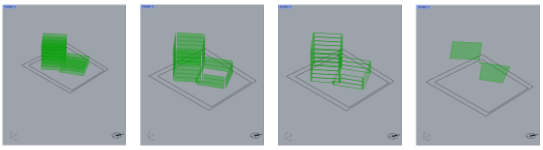

(a) (b) (c) (d)

Figure 7. Parametric adjustments of building mass: floor height, orientation, envelope, and roof components

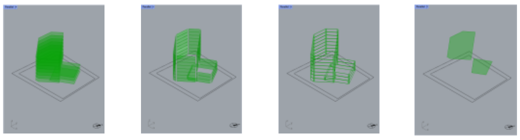

(a) (b) (c) (d)

Figure 8. Parametric adjustments of building mass: floor height, orientation, envelope, and roof components (Automated trimming of excess mass)

To support the generation of multiple building mass configurations, three CSG strategies were applied. Union combines two or more base volumes into a single, continuous geometry. This operation produces compact forms of aggregated volumes, as seen in Figure 9. Subtraction removes one volume from another, producing form defined by the remaining geometry, as seen in Figure 10. Intersection extracts the overlapping volume of two or more solids, generating intersected geometries with reduced extent, as seen in Figure 11. These strategies provide a systematic approach to constructing variants and enable structured manipulation of primitives for analysis (Chen *et al.*, 2025; Ming *et al.*, 2016). (a)Initial base volumes, (b) Alignment and positioning (c), Boolean merging process, (d) Final unified building mass.

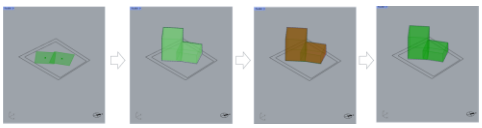

(a) (b) (c) (d)

Figure 9. Solid union operation for generating compact building masses

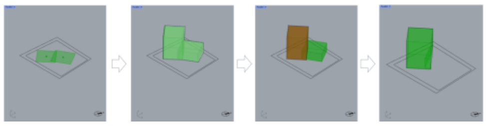

(a) (b) (c) (d)

Figure 10. Solid subtraction operation for generating compact building masses

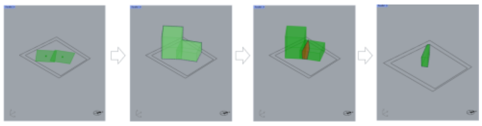

(a) (b) (c) (d)

Figure 11. Solid intersection operation for generating compact building masses

2. Evaluation module

Models meeting criteria proceed to the Evaluation Module, analyzing compliance and OCE. This module checks whether models meet objectives or require refinement. Results are presented in a Pareto-frontier graph, enabling comparison and selection of alternatives based on aesthetics, function, and performance before later phases.

The model of each CSG strategy was assigned a unique identifier and parameter set to facilitate evaluation of building form performance, as seen in Figure 13. The OCE of these configurations was assessed using Climate Studio, a simulation tool that integrates with Rhino and Grasshopper. Following evaluation, models were classified as valid or invalid based on compliance with predefined constraint functions embedded in the optimization framework. The constraint functions also integrated architectural and code requirements such as floor area ratio (FAR), open space ratio (OSR), service core design, and a minimum floor plate area for office design.

For example, GFA must not exceed or be equal to the area specified by FAR regulations, and the building footprint design must comply with the OSR. In addition, the floor plate of each level must be no less than 1,900 m² for open-plan office design, and the service core must be at least 20% of the floor plate or 400 m² per floor. If these fitness functions are not satisfied, the design is penalized and considered invalid. Invalid Type A models have GFA = 1 and OCE = 0. Although these models comply with FAR and OSR constraints, they fail to provide open-plan space or functional layouts, including the service core. Therefore, they are deemed invalid and have no building form displayed. In contrast, Invalid Type B models have

GFA = 0 while maintaining normal OCE, indicating the design exceeded FAR or OSR. As a result, they are penalized: if GFA exceeds FAR, the function sets GFA to zero. This type represents models violating planning regulations such as FAR or failing to meet OSR requirements.

3. Optimization module

Optimization strategies use NSGA-II, incorporating crossover, selection, mutation, and variation to refine models by maximizing GFA and minimizing OCE. Floor area per level is embedded to ensure feasible and compliant solutions. Masses are generated through iterative loops with predefined size and count, applying parametric transformations to align forms with objectives. After generating the building mass, NSGA-II was applied through Wallacei in Grasshopper with two objectives: maximizing GFA and minimizing OCE, as shown in Figure 13. These objectives served as fitness functions to determine building form and shape. Wallacei X runs evolutionary simulations with NSGA-II, integrating multi-objective optimization and clustering techniques, and provides an interface that enables designers to analyze and select optimal solutions from large populations of alternatives. Operating within Grasshopper's environment, it is suitable for early-stage applications such as façade optimization and urban massing. The process produced model configurations based on defined population size and generation count, with outcomes visualized through parameter and data charts and exported to Excel for further analysis.

4. Visualization Module

The Visualization Module presents results through graphs, primarily Pareto frontiers and comparative visualizations, enabling clear interpretation of trade-offs between objectives such as maximizing GFA and minimizing OCE. By illustrating objectives on the Pareto frontier, the module supports informed decision-making and the selection of optimal solutions before detailed stages, thereby enhancing efficiency and usability while bridging analysis with intuitive design insights (Khosakitchalert & Seghier, 2025). It also provides performance metrics and parameters for each configuration, distinguishing valid from invalid models, with valid cases analyzed through a Pareto frontier graph that identified three scenarios: minimum GFA, maximum GFA, and a balanced trade-off between GFA and OCE. The optimal configuration was then selected based on the lowest carbon intensity, as shown in Figure 12. Parameter values of OCE and GFA informed the Pareto frontier analysis, as shown in Figure 12, which shows carbon intensity ($kgCO_2eq/m^2$) and reflects the environmental performance of each solution. This process facilitated decision-making by highlighting the relative performance of CSG strategies, enabling users to compare alternatives under constraints, select the final scheme, and iteratively adjust building shapes to meet requirements during early design.

5. Computational Efficiency Assessments

This section outlines the method for evaluating computational efficiency and design performance of three CSG strategies (union, subtraction, and intersection) during the early design. The evaluation used four criteria: simulation runtime, model validity, design diversity, and carbon intensity (Lin & Gerber, 2014).

First, simulation runtime was measured as total time required for each CSG strategy's simulation. This reflects computational demand and practicality for repeated iterations.

Second, model validity was determined by compliance with zoning and regulatory constraints, including FAR, OSR and height. Constraint functions were integrated into the optimization loop

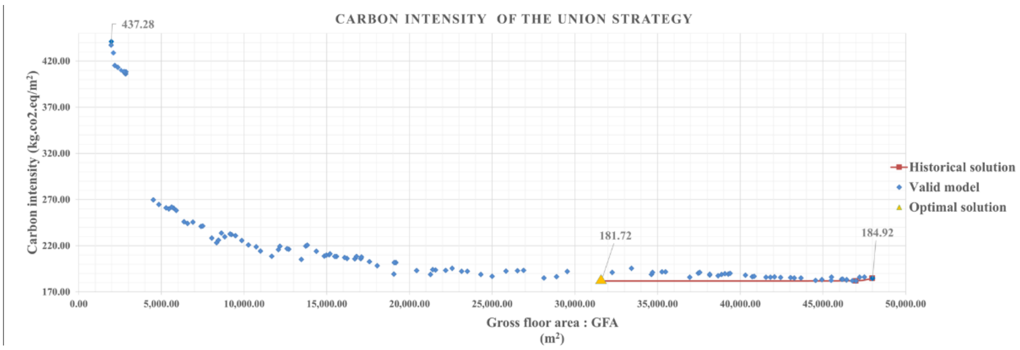

Figure 12. The Pareto frontier analysis was informed by OCE and GFA values in conjunction with data visualizations

to iterate automatically until 1,000 configurations were generated.

Third, design diversity was measured by the number and distribution of valid configurations generated for each strategy. Diversity was assessed using spacing (distance between solutions) and entropy (evenness across design space). Higher entropy reflects greater diversity, while lower entropy suggests indicates concentration of similar designs.

Fourth, carbon intensity ($kgCO_2e/m^2$) was calculated for representative configurations. The analysis considered minimum, maximum, and optimal values of OCE. Optimal solutions balanced minimum OCE and maximum GFA.

To illustrate trade-offs between design and performance, building mass solutions such as minimum GFA, the lowest OCE, and maximum GFA were selected from each strategy's pool. These examples showed how differences affected GFA, OCE and supported identification of the most suitable strategy for reducing iteration time in context-specific scenarios.

Case study

This section presents a case study demonstrating the proposed workflow through a performance-driven massing study on a real urban site in Bangkok, Thailand. The study shows how generative design workflows can support early-stage decision-making by balancing competing architectural objectives.

Site and Environmental Context

This study focuses on a real urban site in the Sathorn district of Bangkok, Thailand, as seen in Figure 13. The site is located in a high-density commercial zone at 13°43′05.0″N, 100°31′53.4″E within a tropical monsoon climate zone by Köppen Am. The designated building type is an office building. The parallelogram-shaped plot is suitable for testing parametric modeling and multi-objective optimization in early-stage mass design, as its non-orthogonal boundaries and spatial constraints reflect the complexity of real urban tissue for building shape optimization experiments. This suitability comes from zoning-compliant conditions that support real-world urban planning regulations, including a maximum FAR of 1:8, a minimum OSR of 40%, a height limit of 273 meters, and required setbacks. These constraints ensure that simulated design scenarios reflect realistic and enforceable conditions.

The site boundary was digitized and used as the base geometry in Grasshopper. Design challenges include limited area, irregular geometry, and surrounding tall buildings. The climate conditions demand careful consideration of shading, ventilation, and daylighting to reduce OCE through building shape design, further supporting the site's selection for evaluating generative design workflows under real-world constraints. Additional building performance parameters were defined for simulation purposes. The WWR was set at 0.90 on all facades. Equipment load was specified as 7 W/m² and lighting load as 16 W/m². Operational schedules were established as follows: Weekdays from 08:00 to 18:00 with variable usage, and no usage on weekends or holidays. Occupancy was set at 0.0714 person/m² under the same weekday schedule, as seen in Table 1 and Figure 13.

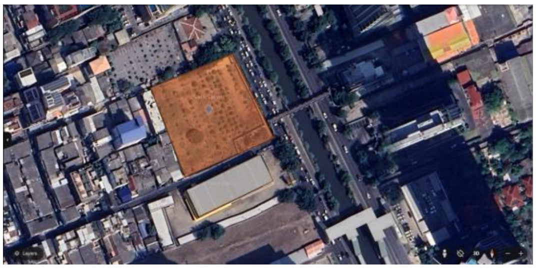

Figure 13. Aerial view of Site 1 (Sathorn) showing urban context and site boundary

Table 1. Shows Programmatic Attributes of the Case Study Building

Type	Details
Glazing Area Ratio	WWR: 0.90 on all facades (N, S, E, W)
Equipment Schedule	7 W/m² Weekdays: 08:00-18:00 (variable usage); Weekends/Holidays: No usage
Lighting Schedule	16 W/m² Weekdays: 08:00-18:00 (variable usage); Weekends/Holidays: No usage
Occupancy Schedule	0.0714 person/m² Weekdays: 08:00-18:00 (variable usage); Weekends/Holidays: No usage

The programmatic attributes of the case study building and the input parameters for the simulation were derived from the default settings available in Climate Studio for office building typologies, since default values improve reliability, support early-stage evaluation of building energy performance, and reduce errors from manual data entry. Internal loads, HVAC configurations, and energy sources were aligned with SIA Merkblatt 2024 (Solemma LLC, 2023). The envelope performance and building systems were configured using predefined templates and the internal database in Climate Studio, as seen in Table 2. Operational schedules and mesh resolution were manually adjusted to ensure compatibility with both energy and daylight simulation requirements, enabling effective evaluation of OCE

Table 2. Thermal and environmental properties of building envelope specified in Assemblies of SIA Merkblatt 2024

Type	Material	Thickness (mm)	Thermal conductivity (W/(m·K))	Density (kg/m^3)	Carbon emission factor	Thermal transmittance (W/(m^2·K))
External wall	Lightweight insulated panel	200	0.2	600	0.12	0.4
Roof	Lightweight insulated roof	300	0.15	450	0.11	0.2
Floor	Concrete slab with insulation	250	0.25	2200	0.13	0.4
Internal wall	Plasterboard on metal stud	125	0.3	800	0.10	1.5
Window	SinglePaneClr	-	-	-	0.5	5.894
Window (Frame)	Aluminum	50	5.0	-	-	-

Table 3. Range variable parameters building mass

Parameter	Range	Unit
MASS1_wlc_BF-X-size =	10.00 to 30.00	m
MASS1_wlc_BF-Y-size =	10.00 to 30.00	m
MASS1_wlc_Position-X-coor =	0.00 to 1.00	-
MASS1_wlc_Position-Y-coor =	0.00 to 1.00	-
MASS1_wlc_Oreintion =	0 to 360	Degree
MASS1_wlc_No. Floors =	10 to 50	Floor
MASS1_wlc_LiftBrep_Z-axis =	1 to 10	Floor
MASS2_wlc_BF-X-size =	10.00 to 30.00	m
MASS2_wlc_BF-Y-size =	10.00 to 30.00	m
MASS2_wlc_Position-X-coor =	0.00 to 1.00	-
MASS2_wlc_Position-Y-coor =	0.00 to 1.00	-
MASS2_wlc_Orentation=	0 to 360	Degree
MASS2_wlc_No. Floors =	10 to 50	Floor
MASS2_wlc_LiftBrep_Z-axis =	1 to 10	Floor

Setup configuration

This simulation was executed on a workstation equipped with an Intel Core i9-13980HX processor (2.20 GHz), 64-bit operating system, x64-based processor, and 32.0 GB of DDR5 RAM. Grasshopper version 1.0.0007 and Wallacei X version 2.6.4 were used to ensure compatibility and computational efficiency throughout the multi-objective optimization workflow.

Design Setup in Grasshopper

The parametric model was developed in Grasshopper 3D. Key geometric parameters, including base dimensions (BF_X and Y), position coordinates (X, Y), building height, number of floors (No. Floors), number of massing elements (MASS 1, 2), vertical movement along the Z-axis (LiftBrep_Z-axis), and orientation were defined as genes using sliders. These parameters were connected to Wallacei X for multi-objective optimization. To generate various building configurations, CSG strategies were employed according to the number of mass elements. The three strategies applied as separate cases: (1) union, creating compact solid volumes; (2) subtraction, generating perforated or carved-out forms; and (3) intersection, producing intersected massing configurations. These strategies provided a structured method for creating spatial diversity in the design process. To ensure a fair and normalized comparison, the parametric boundaries for 'design freedom' were applied consistently across all three CSG strategies. The identical set of genetic parameters and value ranges in Table 3 was used to drive the optimization for three strategies. This established an equitable baseline from which to compare the performance resulting from each strategy's unique topological constraints. Sliders controlled input such as building footprint, position, number of floors, orientation, and façade-specific WWR. Performance objectives including GFA, and OCE were connected to the "Objectives" input in Wallacei X. Simplified geometry was optionally linked to the "Phenotype" input to visualize solutions. Below are the variable ranges in the Grasshopper-Wallacei setup, including geometric and environmental parameters for each mass (MASS1 and MASS2), with a fixed façade-specific WWR of 90% , as seen in Table 3. The parameters and ranges defined (e.g., Number of floors, building footprint dimensions) were selected as they are considered primary drivers impacting both GFA and OCE in early-stage design.

Wallacei X Configuration

Wallacei X operated as an evolutionary engine using NSGA-II. The simulation used a population size of 100 and 10 generations, resulting in 1,000 simulations per strategy. Since three CSG strategies were evaluated, the simulation produced 3,000 simulations. To optimize computational performance, Rhino was minimized to reduce computational load.

Outcome of PA-O-CEE framework

The simulation produced 1,000 unique building mass configurations over 10 generations, each with 100 individuals per the three CSG strategies. This resulted in 3,000 simulations. Each solution was evaluated against key performance objectives: maximizing GFA and minimizing OCE. The results were exported to Excel for post-processing. Subsequently, data were processed into carbon intensity (kgCO_2eq/m²), and Pareto-front plots visualized trade-offs and identified optimal configurations. Representative solutions from each generation were selected to illustrate trends and convergence behavior across generations. Despite convergence in later generations, morphological diversity among the solutions remained, demonstrating the algorithm's capability to balance multiple design goals effectively

Results and Discussion

This study examined the effectiveness of three CSG strategies, namely Union, Subtraction, and Intersection, within a parametric design framework powered by NSGA-II. The focus was on optimizing OCE and GFA in early design. Each strategy was assigned to 1,000 simulations, resulting in 3,000 building mass. The findings reveal computational efficiency between simulation runtime, model validity, design diversity, and carbon intensity, highlighting the role of generative logic in building mass, as seen in Table 4 and Table 5.

Union produced the highest number of valid models (726), suggesting strong geometric robustness under regulatory constraints. However, it showed lower GFA (31,595.78 m²) and the longest simulation time (10h 7m 2s), among the three strategies. While its carbon intensity (181.72 kgCO_2eq/m²) was close to that of Subtraction, its lower form variability may reduce applicability to practical projects.

Subtraction emerged as the most balanced strategy, producing the highest design diversity (151), the largest GFA (45,901.85 m²), and the lowest OCE (181.30 kgCO_2eq/m²). This outcome reflects void-based massing, which expands spatial permutations and promotes improved passive environmental performance. However, the benefits came with moderate runtime (7h 49m 11s), and increased sensitivity to parameter variation, which may affect model stability and repeatability.

Intersection offered the shortest runtime (3h 40m 40s), making it attractive for iterative workflows or rapid prototyping. Nonetheless, it produced the fewest valid models (462) and had the lowest design diversity (112). Its restricted spatial outcomes and reduced GFA (40,359.38 m²) indicate limitations in design flexibility, though its carbon intensity (181.9 kgCO_2eq/m²) remained within an acceptable range.

Although the differences in carbon intensity appear numerically small, the implications are considerable at the building scale. In large developments, even minor improvements in OCE yield substantial annual emission reductions (Röck *et al*., 2020; Torabi *et al*., 2025). Additionally, increased design diversity may enhance long-term adaptability and contribute to lifecycle carbon efficiency (Idrissi Kaitouni *et al*., 2025; Pinich *et al*., 2023; Zhang *et al*., 2024).

Table 4. Optimization efficiency of GFA for the CSG strategies at Sathorn

Mass I.D.	Union mass Gen8_Inv22	Subtraction mass Gen8_Inv12	Intersection mass Gen8_Inv18
	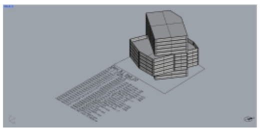	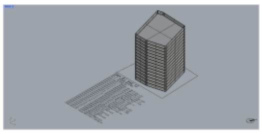	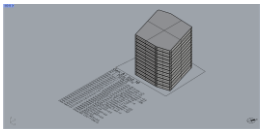
Attribute	The lowest of OCE	The lowest of OCE	The lowest of OCE
GFA: m²	31,595.78	45,901.85	40,359.38
OCE: kg.co_2.eq	5,741,500	8,322,000.00	7,341,800.00
kg.co_2.eq/ m²	181.72	181.30	181.91

Table 5. An evaluation of the computational efficiency of performance algorithms

Computational efficiency/Strategy	Union	Subtraction	Intersection
Simulation runtime (Hours)	10h 7m 2s	7h 49m 11s	3h 40m 40s
Valid model (Number of mass)	726	675	462
Diversity model (Number of distinct form)	120	151	112
GFA of the lowest OCE (m²)	31,595.78	45,901.85	40,359.38
Lowest OCE (kgCO_2eq/m²)	181.72	181.30	181.91

These findings are particularly relevant in dense urban environments, where planning constraints, office design criteria, and regulatory limitations reduce design flexibility (Jang *et al*., 2022; Cruz *et al*., 2024). The subtraction strategy supports both spatial performance and carbon reduction, and could inform future policy mechanisms such as zoning incentives or design regulations for climate-responsive development

This study's scope remains limited, as model validation focused solely on geometric and zoning compliance, excluding structural feasibility, daylight performance, and embodied carbon. For instance, the subtraction strategy, while performing well on OCE, often increases the surface-to-volume ratio, which could potentially increase embodied carbon emissions through greater material use in the façade; an aspect a full LCA would be needed to confirm. To enhance robustness and relevance, future research should include these dimensions and test across diverse climates and regulatory contexts. Sensitivity analysis is recommended to ensure consistency across strategies.

The simulations used a fixed WWR of 0.90 through the PA-O-CEE framework to generate regulation-compliant massing. Operational carbon intensity was calculated using parameters specific to building type and site, including internal loads, thermal demand, lighting, fan systems, and hot water usage. This supports holistic early-stage evaluation and consistent benchmarking (Lin & Gerber, 2014; Kamel *et al*., 2024).

Therefore, selecting a suitable CSG strategy early in design is critical for balancing spatial efficiency and environmental outcomes. Subtraction shows strong potential for low-carbon massing in dense urban settings but requires consideration of computational efficiency and regulatory constraints.

Conclusions

This study demonstrates the effectiveness of the PA-O-CEE framework in generating carbon-optimized building mass configurations through three CSG strategies: union, subtraction, and intersection, within a performance-based parametric workflow. The method applied NSGA-II to perform multi-objective optimization under regulatory constraints such as FAR, OSR, service core ratios, and minimum usable floor area, based on zoning regulations in Bangkok, Thailand. The workflow operates independently of conventional 3D modeling platforms.

The comparison of CSG strategies revealed distinct trade-offs. The union strategy demonstrated the highest model validity, proving most effective at generating geometrically consistent forms that meet regulatory requirements such as FAR and core efficiency. Conversely, the intersection strategy offered the fastest simulation runtime, highlighting its utility for rapid design iteration.

Based on the objectives of this study, the subtraction strategy is recommended as the most effective approach. It emerged as the most balanced solution, successfully achieving the lowest operational carbon emissions while simultaneously producing the highest design diversity. This indicates that subtraction is a highly adaptable strategy for balancing spatial quality and environmental performance, particularly within the complex constraints of dense urban contexts.

However, the current findings may have been affected by differences in design space definitions. Subtraction may have benefited from greater morphological flexibility. A sensitivity analysis is recommended to ensure fairness across strategies under equivalent parametric boundaries, for example, comparing number of floors against setback requirements in high-rise buildings. Notably, subtraction proved to be adaptable for balancing spatial quality and performance in dense urban contexts.

The study focused solely on OCE, using a fixed WWR of 90%, which aligns with typical high-rise office design. This simplification enabled consistent comparison between strategies but excluded ECE considerations and broader Life Cycle Assessment (LCA) impacts. By controlling façade-related variables such as solar gain, thermal transmittance, and orientation responsiveness, the fixed WWR ensured that variations in OCE were primarily attributable to differences in massing geometry, clarify the intrinsic impact of CSG strategies.

Future research should expand the scope in four key areas. First, the optimization criteria should include both OCE and ECE, using LCA as a core metric. Second, design variables should incorporate orientation-responsive WWR, shading devices, and passive systems to enhance thermal and visual performance. Third, the framework should be tested across various building types and climate zones to evaluate generalizability. Fourth, immersive technologies such as Augmented Reality (AR) could be integrated to support participatory design processes and stakeholder engagement.

In conclusion, the PA-O-CEE framework offers a viable approach for carbon-conscious decision-making in early-stage design. It enables optimization that balances regulatory compliance, spatial performance, and environmental targets, particularly in dense urban contexts where sustainable development is most critical.

Acknowledgement

The authors gratefully acknowledge the support of the Thai Government Scholarship for Science and Technology, which provided scholarship support to the first author, Thanasak Phittayakorn, during his studies at Chulalongkorn University.

References

Ahmed, F., Bhattacharya, B., & Deb, K. (2013). Constructive solid geometry based topology optimization using evolutionary algorithm. In J. C. Bansal, P. K. Singh, K. Deep, M. Pant, & A. K. Nagar (Eds.), *Proceedings of Seventh International Conference on Bio-Inspired Computing: Theories and Applications (BIC-TA 2012)* (pp. 227-238). Springer India. https://doi.org/10.1007/978-81-322-1038-2_20

Ahmed, F., Deb, K., & Bhattacharya, B. (2016). Structural topology optimization using multi-objective genetic algorithm with constructive solid geometry representation. *Applied Soft Computing*, *39*, 240-250. https://doi.org/10.1016/j.asoc.2015.10.063

Alkadri, M. F., De Luca, F., Turrin, M., & Sariyildiz, S. (2020). A computational workflow for generating a voxel-based design approach based on subtractive shading envelopes and attribute information of point cloud data. *Remote Sensing, 12*(16), 2561. https://doi.org/10.3390/rs12162561

Broyles, J. M., Gevaudan, J. P., Hopper, M. W., Solnosky, R. L., & Brown, N. C. (2024). Equations for early-stage design embodied carbon estimation for concrete floors of varying loading and strength. *Engineering Structures*, *301*, 117369. https://doi.org/10.1016/j.engstruct.2023.117369

Chen, Y., Liu, Y., & Kayar-Ceylan, G. (2025). CSG-based ML-supported 3D translation of sketches into game assets for game designers. *The Visual Computer, 41*(8), 5891-5903. https://doi.org/10.1007/s00371-024-037

Churkina, G., Organschi, A., Reyer, C. P., Ruff, A., Vinke, K., Liu, Z., Reck, B. K., Graedel, T. E., & Schellnhuber, H. J. (2020). Buildings as a global carbon sink. *Nature Sustainability*, *3*(4), 269-276. https://doi.org/10.1038/s41893-019-0462-4

Ciardiello, A., Rosso, F., Dell'Olmo, J., Ciancio, V., Ferrero, M., & Salata, F. (2020). Multi-objective approach to the optimization of shape and envelope in building energy design. *Applied Energy*, 115984. https://doi.org/10.1016/j.apenergy.2020.115984

Cruz, C., Caldas, L., Mendes, A., Mendes, J., & Bastos, P. (2024). Multi-objective optimization based on surrogate models for sustainable building design: A systematic literature review. *Building and Environment*, 112147. https://doi.org/10.1016/j.buildenv.2024.112147

Deb, K., Pratap, A., Agarwal, S., & Meyarivan, T. (2002). A fast and elitist multiobjective genetic algorithm: NSGA-II. *IEEE Transactions on Evolutionary Computation, 6*(2), 182-197. https://doi.org/10.1109/4235.996017

Dunant, C. F., Drewniok, M. P., Orr, J. J., & Allwood, J. M. (2021). Good early stage design decisions can halve embodied CO2 and lower structural frames' cost. *Structures, 33*, 343-354. https://doi.org/10.1016/j.istruc.2021.04.033

Feito, F. R., Ogayar, C. J., Segura, R. J., & Rivero, M. A. (2013). Fast and accurate evaluation of regularized Boolean operations on triangulated solids. *Computer-Aided Design, 45*(3), 705-713. https://doi.org/10.1016/j.cad.2012.11.004

Guo, Y., Wang, H., Cao, Y., & Long, Y. (2023). A new optimization design method of multi-objective indoor air supply using the Kriging model and NSGA-II. *Applied Sciences, 13*(18), 10465. https://doi.org/10.3390/app131810465

Huang, Y. F., Wu, C. Y., Liu, H. C., Meng, L. C., & Zhu, Q. (2020). Integration of constructive solid geometry and boundary representation (CSG-BRep) for 3D modeling of underground cable wells from point clouds. *Remote Sensing, 12*(9), 1452. https://doi.org/10.3390/rs12091452

Idrissi Kaitouni, S., Gargab, F., Es-sakali, N., Mghazli, M. O., El Mansouri, F., Jamil, A., & Ahachad, M. (2025). Digital workflow for nearly zero-energy high-rise office building design optimization at the district scale in Mediterranean context. *Energy and Built Environment*, *6*(6), 1025-1038. https://doi.org/10.1016/j.enbenv.2024.04.008

Jang, S., Yoo, S., & Kang, N. (2022). Generative design by reinforcement learning: Enhancing the diversity of topology optimization designs. *Computer-Aided Design, 146*, 103225. https://doi.org/10.1016/j.cad.2022.103225

Kamel, M., Pittau, F., Dal Verme, F., Scatigna, M., & Iannaccone, G. (2024). A parametric integrated design approach for life cycle zero-carbon buildings. *Sustainability, 16*(5), 2001. https://doi.org/10.3390/su16052001

Kanyilmaz, A., Dang, V. H., & Kondratenko, A. (2023). How does conceptual design impact the cost and carbon footprint of structures? *Structures, 58*, 105102. https://doi.org/10.1016/j.istruc.2023.105102

Khosakitchalert, C., & Seghier, T. E. (2025). Evaluating and optimizing acoustical reverberation time and material cost for classrooms using building information modeling (BIM) and generative design (GD) tools. *Nakhara: Journal of Environmental Design and Planning, 24*(1), Article 504. https://doi.org/10.54028/NJ202524504

Lin, S.-H. E., & Gerber, D. J. (2014). Designing-in performance: A framework for evolutionary energy performance feedback in early stage design. *Automation in Construction, 38*, 59–73. https://doi.org/10.1016/j.autcon.2013.10.007

Lu, Y., Wu, Z., Geng, Y., Liu, Y., Zheng, X., & Hou, H. (2022). Multi-objective optimization of building environmental performance: An integrated parametric design method based on machine learning approaches. *Energies, 15*(19), 7031. https://doi.org/10.3390/en15197031

Mews, M., Aynetdinov, A., Schiller, V., Eisert, P., & Akbik, A. (2024). *Don't mesh with me: Generating constructive solid geometry instead of meshes by fine-tuning a code-generation LLM. arXiv*. https://arxiv.org/abs/2411.15279

Ming, X., Yanzhu, H., Jianguang, W., & Yong, Z. (2016). A topological enabled three-dimensional model based on constructive solid geometry and boundary representation. *Cluster Computing, 19*(4), 2027-2038. https://doi.org/10.1007/s10586-016-0634-1

Parasonis, J., Keizikas, A., & Kalibatiene, D. (2012). The relationship between the shape of a building and its energy performance. *Architectural Engineering and Design Management, 8*(4), 246-256. https://doi.org/10.1080/17452007.2012.675139

Pinich, T., Srimuang, W., & Sreshthaputra, A. (2023). Optimization of envelope heat gain and interior daylight illuminance in building facade design under reflectance limitations: A case study of office buildings in Thailand. *Nakhara: Journal of Environmental Design and Planning, 3*, 1-15. https://doi.org/10.54028/NJ202322317

Röck, M., Saade, M. R. M., Balouktsi, M., Rasmussen, F. N., Birgisdottir, H., Frischknecht, R., *et al*. (2020). Embodied GHG emissions of buildings: The hidden challenge for effective climate change mitigation. *Applied Energy, 258*, 114107. https://doi.org/10.1016/j.apenergy.2019.114107

Schwartz, Y., Raslan, R., Korolija, I., & Mumovic, D. (2021). A decision support tool for building design: An integrated generative design, optimisation and life cycle performance approach. *International Journal of Architectural Computing, 19*(3), 401-420. https://doi.org/10.1177/1478077121999802

Shapiro, V., & Vossler, D. L. (1991). Construction and optimization of CSG representations. *Computer-Aided Design, 23*(1), 4-20. https://doi.org/10.1016/0010-4485(91)90095-E

Shen, Y., Wang, Q., Zhang, Y., Tong, Y., & Ji, Y. (2021). EvoMass + GH_Wind: An agile wind-driven building massing design optimization framework. In *Proceedings of the International Conference on Education and Research in Computer Aided Architectural Design in Europe* (pp. 477-486). https://doi.org/10.52842/conf.ecaade.2021.1.477

Shi, Y., Yang, X., Zheng, Y., Gao, Y., & Yang, L. (2025). Multi-objective optimization of embodied carbon emission, energy consumption, and daylighting performance of educational building in the schematic design stage. *Journal of Building Engineering*, 112594. https://doi.org/10.1016/j.jobe.2025.112594

Solemma LLC. (2023). *Climate Studio* [Computer software]. https://www.solemma.com/ClimateStudio

Torabi, N., Simonen, K., & Evins, R. (2025). What matters the most in designing low-carbon buildings in Canada? Exploring the tradeoff between embodied and operational carbon in early stage design. *Energy and Buildings*, 115482. https://doi.org/10.1016/j.enbuild.2025.115482

Wang, L., Janssen, P., & Ji, G. (2024). Optimization-based design exploration of building massing typologies—EvoMass and a typology-oriented computational design optimization method for early-stage performance-based building massing design. *Frontiers of Architectural Research, 13*(6), 1400-1422. https://doi.org/10.1016/j.foar.2024.06.001

Wang, Q. (2022). Workflow for applying optimization-based design exploration to early-stage architectural design: Case study based on EvoMass. *International Journal of Architectural Computing, 20*(1), 41-58. https://doi.org/10.1177/14780771221082254

Wang, Q., Zhang, Y., & Bernard, M. D. (2021). A constructive solid geometry-based generative design method for additive manufacturing. *Additive Manufacturing, 46*, 101952. https://doi.org/10.1016/j.addma.2021.101952

Wang, Z. (2021). *Constructive generative design methods for qualified additive manufacturing* (Doctoral dissertation, École Centrale de Nantes).

Yang, Y., Wang, Q., & Cimillo, K. (2024). Design factor-oriented life-cycle energy optimisation for early-stage building design. In *Proceedings of the International Conference on Computer-Aided Architectural Design Research in Asia* (pp. 465-474). https://doi.org/10.52842/conf.caadria.2024.1.465

Zhang, Y., Wang, Q., Du, J., Tian, Y., Jia, H., Ye, Y., *et al*. (2024). A systematic review of urban form generation and optimization for performance-driven urban design. *Building and Environment*, 111269. https://doi.org/10.1016/j.buildenv.2024.111269